Spring 2022

Water Based Soil Fluidization using a Soft Eversion Robot

James E. Hand
Embry-Riddle Aeronautical University, handj6@my.erau.edu

Water Based Soil Fluidization using a Soft Eversion Robot

by

James E. Hand

A thesis submitted in partial fulfillment of the requirements for the degree of

Master of Science in Unmanned and Autonomous Systems Engineering

at Embry-Riddle Aeronautical University

Department of Electrical Engineering and Computer Science

Embry-Riddle Aeronautical University

Daytona Beach, Florida

May 2022

Water Based Soil Fluidization using a Soft Eversion Robot

by

James Hand

This thesis was prepared under the direction of the candidate's thesis committee chairman, Dr. Christopher Hockley, Department of Mechanical Engineering, and has been approved by the members of the thesis committee. It was submitted to the Department of Electrical Engineering and Computer Science and was accepted in partial fulfillment of the requirements for the degree of Master of Science in Unmanned and Autonomous Systems Engineering.

THESIS COMMITTEE

_____
Christopher Hockley, Ph.D.
Committee Chairman

_____
Brian Butka, Ph.D.
Committee Member

_____
Monica Garcia, Ph.D.
Committee Member

_____ _____
Radu F. Babiceanu, Ph.D. Date
Chair, Electrical Engineering and Computer Science

_____ _____
James W. Gregory, Ph.D. Date
Dean, College of Engineering

_____ _____
Christopher Grant, Ph.D. Date
Associate Vice President for Academics

Acknowledgments

I would like to thank my family, friends, and girlfriend, Alexis Tucker, for pushing me to pursue even higher goals than I ever thought I would reach. Without your support this would be an impossible journey.

I would like to thank Dr. Richard Stansbury for being a wonderful advisor and manager during my time in his research group.

I would like to thank Alex Smith for helping me in the lab, even if it meant getting water and sand all over the both of us.

I would like to thank Dr. Christopher Hockley and Dr. Brian Butka for being wonderful thesis advisors. Their work kept me on task, on time, and challenged me to look deeper.

I would also like to thank all of the other faculty who have mentored, guided, and worked with me throughout my years at Embry-Riddle.

Table of Contents

List of Figures

List of Tables

1 Abstract

Soft robotics, a form of robotics that incorporates nonrigid components, continues to grow in scope, system design, and application. A recent addition to this field is the Vine Robot platform, a bio-inspired robot designed by Stanford University in 2017 [1]. Its method of movement, known as eversion, closely resembles the way that a vine grows along a tree, giving it its name. The focus of this research was to take its proven abilities of underwater vine-like movement and soil fluidization, a process where granular materials are converted from a solid-like state to a fluid-like state, to create an underwater eversion robot capable of burrowing into sand. This was done with the goal of providing a future platform for research into soil composition studies, underwater movement using multiple eversion and fluidization tubes, and other ventures. The unique ability of this platform is extending its reach far beyond that of comparable sized systems [1]. Specific focus was given to the measured abilities of eversion into granular substances using a combination of air and water eversion material, with the former given preference due to its accessibility in underwater environments. The resulting testing showed the capability of using the water as a fluidization material, especially in underwater environments.

2 Introduction

Soft robotics is an ever-growing field that encompasses a large variety of platforms, each with their own unique benefits and drawbacks. One of the many key uses of soft robotics, when compared to their more traditional counterparts, is the ability to maneuver in unique ways. For example, this system has been designed to explore wiring conduits, maneuver underneath large containers, and navigate coral reef systems [1] [2]. It is this unique maneuverability that prompted the work displayed in this paper.

The focus of this research, and its related works, is on the continuation of two specific previous works that in their own way focus on the use of the soft robotic systems. Particularly the Vine Robot platform is the basis for the two previous works mentioned, as well as the research presented in this paper [1]. Specifically, these two papers, created by Naclerio et al. and Luong et al., demonstrate two separate uses of the Vine Robot platform [3] [2].

The first, by Naclerio et al., showcases the robot's ability to house an air-based fluidization system, a system that induces a fluid like state in a granular material using air pressure [3]. In turn this fluidization was used to allow the robot to perform eversion, a system of movement characterized by pushing an inverted tube inside out using air pressure. Luong et al.'s research focuses on a separate use case, the ability to use the Vine Robot system underwater using water as a pressure inducing material in eversion in contrast to compressed air [2].

3 Relevant Background

3.1 Literature Review

The Vine Robot platform originated from Stanford University in 2017 as the product of research conducted in soft robotics [1]. It is described as an inverted tube, typically in the form of plastic or fabric, which can be pressurized to grow outward from its origin point. This is done

only from the tip of the system, as the previously everted sections of tube stay in place. Its resulting movement is typically seen as resembling the way a vine grows up a tree, leading to its namesake.

Original work on this platform focused on the modeling and understanding of how eversion, the system by which air is used to turn tubing inside out to create movement, could be used as a form of locomotion. The original article by Hawkes et al. [1] speaks first on the ability to use pneumatics to evert a material. Secondary to this is the development of control systems for this eversion as it pertains to direction. A large focus of research in the following years investigated other ways to direct, steer, or otherwise control the movement of the Vine Robot system [4]. A large majority of these control systems focused on the use of separate eversion tubes working together in some form to create differing levels of eversion, thus creating a movement in a certain direction of the overall eversion [5]. This is achieved by using two eversion tubes, typically inside of a 'host' tube, that evert using their own control systems. These two control systems allow for varying levels of eversion for each tube, the difference of which can create a change in the 'host' tube direction by applying pressure at an angle between the two pressures.

Moving into 2018 and beyond the focus of most research shifted from control schemes for these platforms to their use to deliver or contain secondary systems. The use of this system as a supplement for inspection purposes, medical research, and industrial processes became very popular. Specific use cases include deployable antennas [6], soft catheters for surgery [7], and the lifting of large uniform objects. The latter was achieved by sliding the robot underneath the object and increasing the pressure inside the eversion tube, creating a lift force underneath the object.

In particular two specific projects relate directly to the current research, sourced from Naclerio's and Luong's papers. The first, by Naclerio's research group [3], dives into the use of the Vine Robot for burrowing into sand using air as a fluidization material. Their assumption, which was ultimately proved correct, was that it was possible to use the eversion of the robot to push into sand, with the help of a secondary tube for fluidization. This secondary tube was sealed inside of the eversion tube, allowing it to grow with the eversion tube that constituted the Vine Robot. Notably, this project mentions the idea of using a different fluidization material for future research, specifically the use of water. Thus, the use of water as a material is something that could satisfy both the use of eversion and fluidization.

Luong et al [2] presents this use of water as an eversion material in their paper, which focuses on underwater usage of the Vine Robot platform. The natural buoyancy induced by air inside a vessel of any kind underwater provides an inherent difficulty. This requires the use of a fluid with a density equal to, or greater than, the density of surrounding fluid for any meaningful use of the platform underwater. Specifically for environmental in an underwater environment, such as the sea or in a lake, it is practical to use the surrounding fluid as an eversion material. As such, this group created, and tested, a version of the Vine Robot capable of using water as an eversion material. To control movement of the eversion tube an internal stepper motor was used to allow for the eversion tube to extend and retract in connection with the internal water pump. In addition, a pressure relief valve was needed to deal with the change in pressures inside of the robot given the incompressibility of water. This was needed as the water pump provided water from outside of the pressure chamber to produce eversion, creating possible pressure differences.

The goal of this research is to combine these two specific research focuses into one exploratory focus. Specifically, this project took the fluidization power proven by Naclerio et al.

and proved the capability of using water as a fluidization material [3]. In addition, this research studied the ability to perform these tasks in an underwater environment.

This research was meant to provide a path for future research to further develop the capabilities of the Vine Robot using fluidization material other than pressurized air. While Luong et al. [2] showed the first use case of this idea, this research hoped to provide an additional use case for this practice. In addition, this research bridged the gap that Naclerio et al. laid out as a possible future research goal by testing the use of water as a fluidization fluid [3].

4 Methodology

4.1 Exploratory Research Outline

Research was conducted in a variety of stages for this project. Planning stages of the project listed several steps in design and testing milestones. First a survey of existing literature and design practices was completed for the specific Vine Robot design created by Naclerio et al. [3]. Once a thorough understanding of the previous design was completed, three separate iterations of the Vine Robot system were created for testing and characterization purposes. This process was iterative, starting with a fully air-based system for both eversion and fluidization. The iteration after this system used water as a fluidization material, while still using an air-based eversion material. Finally, a fully water-based system was created to showcase underwater feasibility of the system and to conduct numerical characterization of the system's interactions with the underwater environment. This combination of water based eversion and fluidization was the first example of such a system at the time of writing.

4.2 Air Induced Eversion and Fluidization Design

The first priority was testing the ability to fluidize sand with air pressure, as performed by Naclerio et al [3]. This was done to gain firsthand knowledge and experience in the use of Vine Robots. To attain this knowledge the researcher created a simply designed version of the Vine Robot, the instructions of which can be found on the Vine Robot website [8]. This version of the platform involves a single airline meant to add air pressure into the system, with a DC motor inside of the pressure chamber to control eversion length. To accomplish this the DC motor was attached to a spool which contained the eversion line. This design does not include any fluidizations designs as it is meant as a basic Vine Robot platform. The completed version of this design can be seen in Figure 1.

Figure 1: Original Design

Testing with this platform showed that the system had several key issues. The first and foremost issue was the fact that the spool and DC motor set up created following these instructions resulted in a misaligned system. The misalignment created difficulties in eversion

control, both in eversion and retraction. This was especially evident when buckling issues in the eversion line became evident, an issue known to plague the Vine Robot platform [9]. Buckling of this type can occur for a variety of reasons, with unequal levels of stress force incurred by different points of the eversion tube being the primary cause [9]. The reasoning for this can be due to differing material strength in the eversion tube, a pulley assembly that is pulling at an angle due to misalignment, or other causes. A secondary, and persistent, issue was the lack of an airtight seal in sections such as the lid of the container. However, work on this platform did provide the needed understanding for the platform moving forward.

To test with air fluidization the DC motor and spool were removed from the container. The reasoning for this was the fact that control was deemed secondary to proof of concept. Thus, a shortened eversion tube was used that could be easily stored inside of the container with little wrapping. A smaller fluid-tube was sealed into the end of the eversion tube, the section of the tube that would be the last to evert, with an impulse heat sealer. This machine uses electrically induced heat to seal two plastic components together. In addition, a liquid adhesive was used to seal any additional gaps left after the impulse heat treatment. This created a sealed line from an external air supply, through the fluid-tube, and into the naturally occurring tube created by the eversion tube.

An example of fluidization line connections and behavior can be seen in Figure 2, Figure 3, and Figure 4. The black line in each image was applied to better visualize the edge of the eversion tube. In practice on a Vine Robot system this would be the connecting point of the eversion tube and robot body.

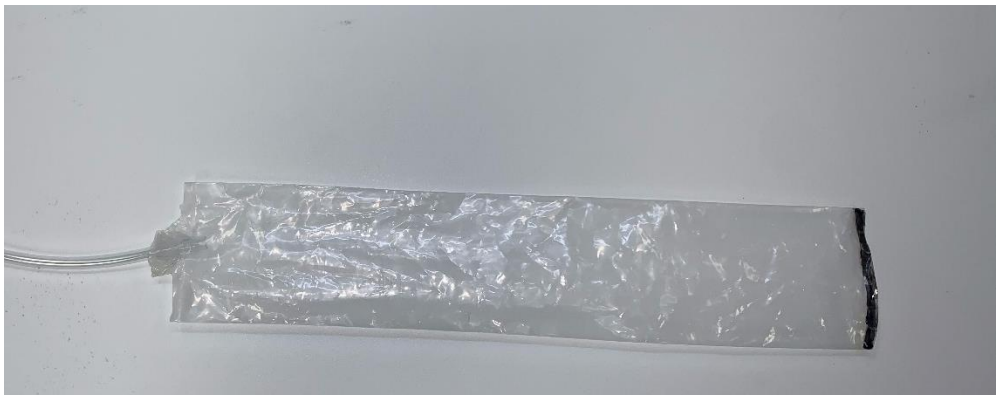

Figure 2: Fluidization Example - No Eversion

Figure 3: Fluidization Example - Half Eversion

Figure 4: Fluidization Example - Full Eversion

The result of this testing achieved soil fluidization, but the lack of a specialized tip meant that the fluidization was inefficient. Due to the nonuniform outlet of the fluidization tube, created as a byproduct of eversion tube structure, the compressed air of the fluidization tube was not

distributed evenly. This resulted in parts of the fluidization tube outputting more of the compressed air than others, with variations based on the structure of the eversion tube at the time of output. With the eversion tube creating the fluidization outlet the pressure of the fluidization tube also varied with the structure, increasing or decreasing the output pressure based on the fluidization opening.

This system was tested in both dry sand and sand under a varying depth of water, typically a minimum of three inches. Fluidization in an underwater environment proved to be easier to achieve. It is likely that this is because the underwater environment reduced the compaction friction that dry sand inherently has.

4.3 Air Induced Eversion with Water Induced Fluidization Design

After the successful proof of fluidization using the air-centric system, focus shifted to using water as the fluidization material, the main goal of this research. To change the design to feature this new fluidization technique the external air supply had to change to a water-based one. Given the type of tubing used for this project the switch only involved using a standardized water spicket attachment with an additional tubing connector. With this change in the design the ability to use water as a fluidization material was possible. The new system design can be seen in Figure 5.

Figure 5: Design of Air System with Water Fluidization

Testing with this design involved a container of sand, submerged beneath a layer of water. The reasoning for the submerging the sand in water was due to the inherent introduction of water by the newly designed system. A testbed starting with dry sand would quickly become damp, and eventually submerged, because water was being introduced into the testbed as it was output from the fluidization tube. This water would result in changes to the properties of the material being everted into. This change in material would result in varying eversion results as a byproduct of initial starting moisture. Thus, only testing in a sand bed covered in a minimum of two inches of water was conducted.

The result of this testing showed that soil fluidization using water as a fluidization material was possible. Initial testing, using an unmeasured waterflow from a standard U.S. water spicket into the fluidization tube, resulted in highly active fluidization of the sand medium. Numerical classification of this success is discussed in Section 5.2. This discovery proved the

general thesis that led this research, prompting further research to attempt both a numerical classification of this fluidization and the use of this fluidization in an underwater focused Vine Robot.

4.4 Water Induced Eversion and Fluidization Design

Following the secondary validation step completed in the form of water-based fluidization, research shifted to the full design of a water centric Vine Robot. Still using the same chamber as outlined in the original construction document, with the key difference between this design and previous iterations being the switch from a pneumatic eversion line. Various water centric design ideas were considered for manufacture and testing. However, some designs would require a complex pressure-tight system, using interlocking seals and custom designed chamber features. In the goal of creating a system easily managed and maintained by one operator these requirements were determined to fall outside of the scope of this project. Given these constraints a simpler design was kept, however, the basic schematic for one of these vetoed projects can be seen below in Figure 6.

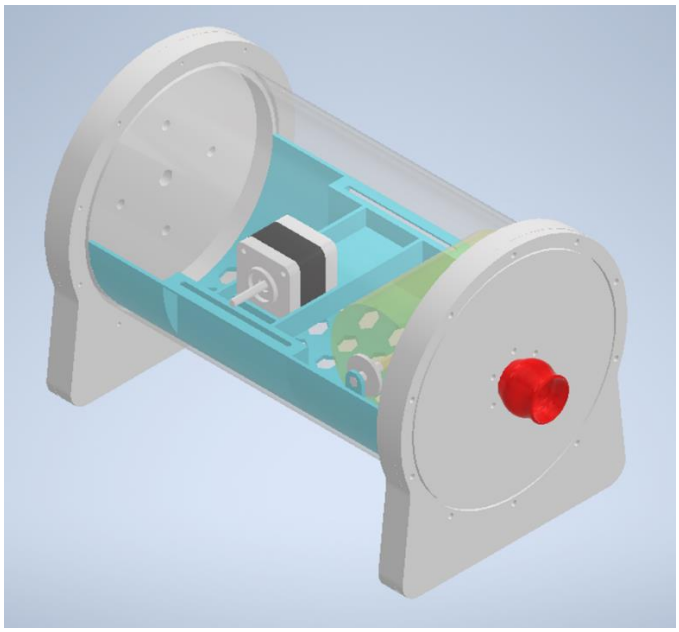

Figure 6: Water Centric Design Idea

A chief concern with the design seen in Figure 6 was the complex pressure and control systems would introduce possible variables to testing. Any future work should incorporate a variation of these designs to provide a more accurate, reliable, and contained system. Figure 6 is designed after the same system used by Luong et al, given its proven abilities in underwater environments [2]. Planned additions would include a secondary spool mechanism to hold the fluidization line. This addition would be required to maintain control over the fluidization tube, as well as allow it proper access to the 'end' of the eversion tube which is typically connected to the pulley system first.

To achieve this connection between the two lines the spool of the eversion line would be hollow. One side of the eversion spool would be the connection point for the eversion control motor while the other allowed the fluidization line to connect to the spool. To avoid twisting the fluidization line as the eversion spool moves the line and spool would be connected using a sealed ball bearing connector, similar to a flange bearing. While this would leave the eversion and fluidization lines disconnected it would still allow the fluidization line to transfer water pressure into the hollow spool which would escape through the connection the eversion line has to the spool. A basic CAD model of this spool design can be seen in Figure 7.

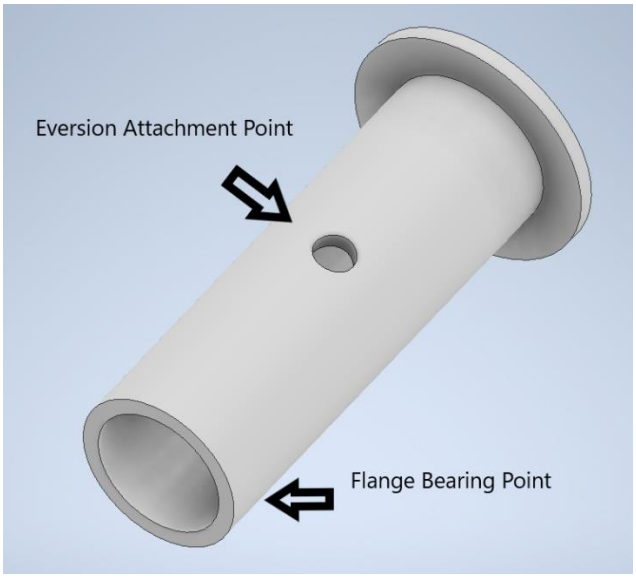

Figure 7: Spool Design

The design chosen for testing purposes was, as mentioned previously, a variation of the original preformed Vine Robot design provided by Zepeda [8]. A connector assembly was added to allow access to the internally stored fluidization line. The was created to ensure a pressurized interior chamber while still having access to the fluidization line. In addition, the original eversion line was kept, but reinforced with adhesive to limit fluid escaping from the chamber.

The internal motor, which operated the eversion line spool system, from the original design was kept out of the system, due to a variety of factors ranging from safety and mechanical alignment issues. Running electrical wiring through the water system was deemed a safety risk, due to the chance of electrical shock to the operator. Additionally running a DC motor in an underwater environment can quickly lead to corrosion or grounding issues.

This left the system controlled solely by water eversion pressure, which presented similar challenges and abilities to that of a controlled system. A full picture of the final design can be seen in Figure 8.

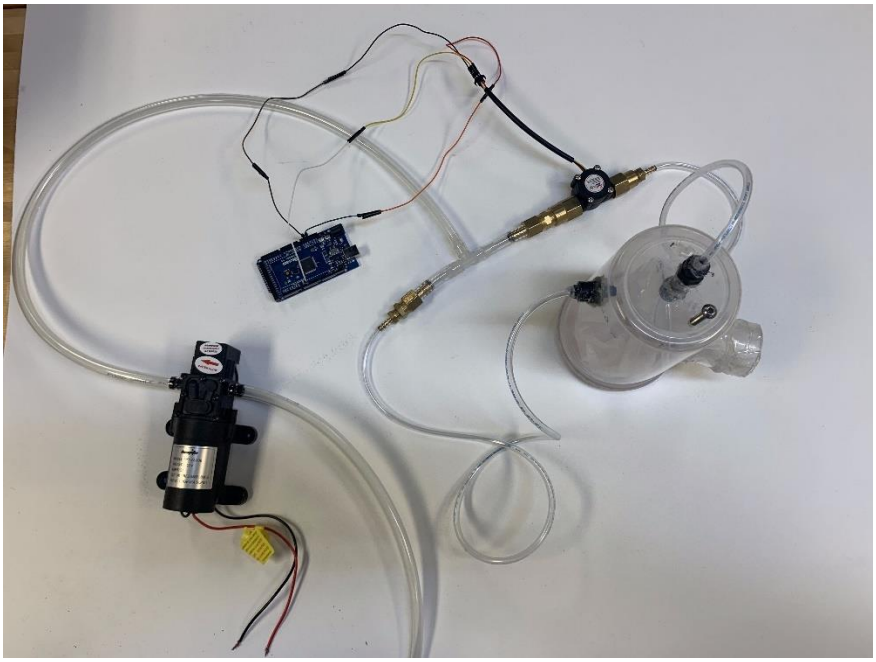

Figure 8: Full Water Based Design Implementation

The system's water supply was powered by a 12-volt DC electric water pump, connected to an external power supply. Water was filled into a large grade industrial container, five gallons in volume, which could be drawn into the pump when activated. The outlet of the pump entered a 'T' junction connector, splitting the water between both the eversion and fluidization lines. The eversion line led directly into the pressure chamber, while the fluidization line passed through a water flow meter before moving into the connecting system, and finally into the fluidization line attached to the eversion tubing. Output of the waterflow sensor was logged at a rate of once per second during operation. A detailed view of the water flow connections can be seen below in Figure 9 and the wiring for the water flow sensor can be seen in Figure 10.

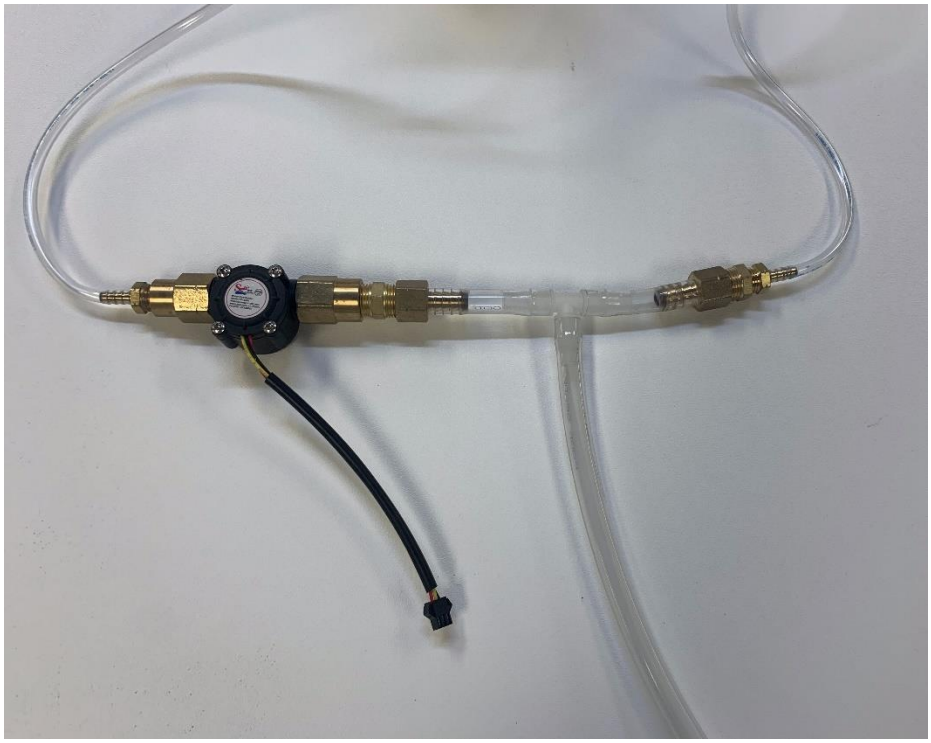

Figure 9: Water Flow Connections

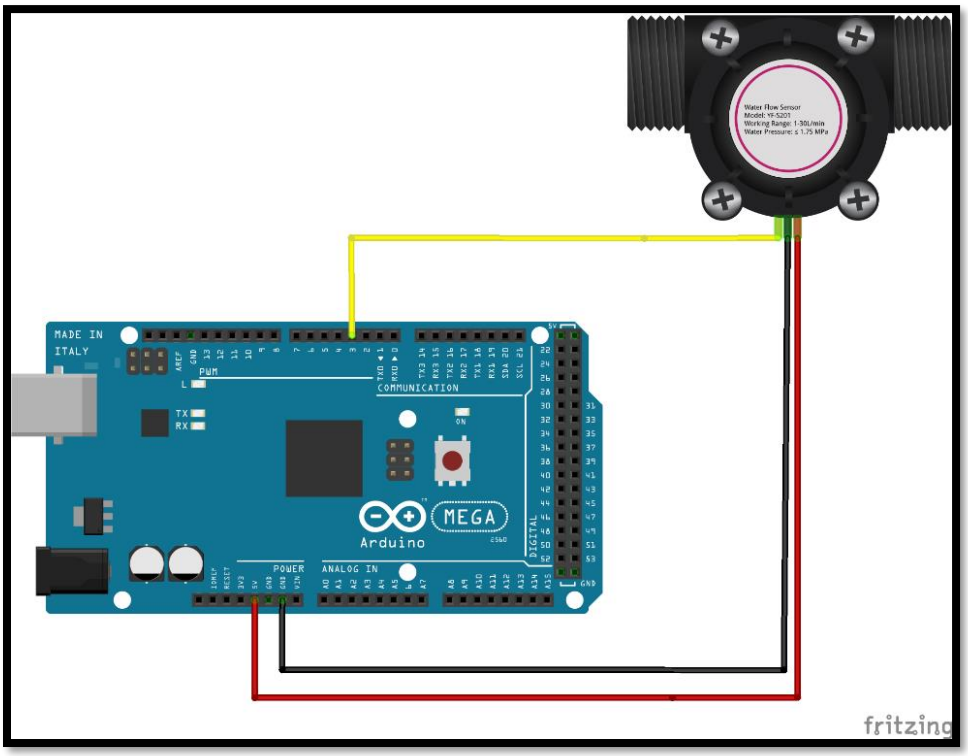

Figure 10: Water Flow Sensor Wiring

4.5 Testing of Water Centric Design

Testing with the new design was done in two different stages, control studies and sand eversion testing. To conduct these tests a testbed was created using a large storage container (21.5in x 15in x 12.5in), filled evenly with six and a half inches of beach sand. Initial testing was conducted with no water introduced beforehand, meaning that any water in the system came directly from the fluidization line. With loose dry sand this showed some success, which will be discussed in Section 5.1. However, once the sand became damp the eversion became far more difficult, resulting in slower eversion rates. This discovery led to the introduction of water before testing, three inches in depth above the sand line. With the introduction of water prior to testing the difficulty in achieving eversion was removed.

Following this, timed testing trials began, starting with a horizontal test of eversion. This required the burying of the robot into the sand medium, typically such that the eversion tube line would be under three inches of sand. The idea behind this testing would be to test over longer eversion lengths, tracking the time required for sufficient eversion.

However, this proved to be a far more difficult form of testing. The time required to fill the pressure chamber, bury the system, measure sand depth, and run the eversion test resulted in each trial run taking upwards of twenty minutes to produce reliable data. In addition, this horizontal motion resulted in the eversion line trending upwards, growing out of the sand medium within a short period of time. This led to results that focused less on the eversion and fluidization characteristics of the robot and more on the characteristics of the soil covering the path the eversion line took. The amount of sand over the length of this horizontal motion would need to be exactly the same, otherwise it would introduce different levels of pressure from above

from both the sand and the water above the sand. See Section 5.1 for further discussion on these results.

Figure 11: Horizontal Orientation Testing

These observations led to a change in testing philosophy, and a change to the testbed. Instead of a horizontal orientation the system was oriented vertically so that the eversion tube was facing towards the sand from above. This was achieved by placing tube PVC rods through the indentations of the testbed container and securing them with adhesive tape. This provided a fixed position above the sand for the system to repeatedly operate from. To prevent the system from shifting during eversion due to torque, or other outside forces, a foam piece was affixed to the tubing to act as a fixed point. This elevation above the sand typically resulted in four-and-a-half-inch gap between the eversion tube exit from the system and the sand of the testbed, with variations resulting from differing sand height. This new system of testing can be seen in Figure 12.

Figure 12: Vertical Orientation Testing

With this final testing system assembled, additional time trials were completed to begin gathering data to classify the ability of eversion into submerged sand using water as a fluidization material. In addition, a series of trials were completed with the robot system orientated in the same manner with no sand medium present beneath it, labeled as control studies. This was done to complement the sand eversion trials, providing a numerical comparison between eversion in open air and sand mediums. The results of these trials will be discussed in Section 5.2.

To create a better understanding of the water pump and water flow characteristics, a test was conducted without the system drawing water. The robot was disconnected from the water pump system and the 'T' connector was sealed on one side so that all water output was sent through the water flow sensor. This was done three times, with each trial lasting sixty seconds. These three sets of data were averaged together to receive a total average water flow rate, measured to be in the order of 233 [L/Hour], with a ± 2% error margin in sensor reading. However, it is important to note that this testing does not involve the backpressure that can be present in the testing system. As sand pushes against the eversion arm during eversion, there is the chance for backpressure to be induced in the system. This pressure could, in theory, cause

changes in water output and distribution. Future work could include a more in depth look into the affects of pressure on water output and distribution as it relates to external pressure.

```
%Load water test values
w1 = table2array(readtable("WaterTestRun1.txt"));
w2 = table2array(readtable("WaterTestRun2.txt"));
w3 = table2array(readtable("WaterTestRun3.txt"));

%Average of each water test
w1ave = mean(w1(:,2));
w2ave = mean(w2(:,2));
w3ave = mean(w3(:,2));

%Average of all water tests
wave = (w1ave+w2ave+w3ave)/3;
```

Figure 13: Water Flow Rate Averaging

5 Results

5.1 Testing Outcomes

Initial testing results with dry sand worked as described in Naclerio et al.'s paper on air-based fluidization [3]. The lack of a specialized tip for this testing resulted in unpredictable levels of fluidization, however, this stage in testing was meant as a proof of concept before further research. No data was collected for these trials due to their proof-of-concept nature.

As mentioned previously, the switch to a water-based fluidization scheme provided additional challenges compared to that of the air-based system. The introduction of water into the dry sand proved to be a challenge until sufficiently submerged. Eversion using dry sand and water-based fluidization resulted in the sand congealing together. This resulted in the individual particles sticking together, creating larger 'chunks' of material to be moved by the fluidization

water. These larger particles required more force to fluidize, resulting in poor performance until enough water was in the testbed to facilitate increased granular movement.

This performance is similar to the research compiled by Fiscina and Wagner in their study focused on wet and dry sand flow characteristics [10]. This study showed that water, when introduced to sand, can change the flow characteristics between granules. A notable increase in structural integrity was observed in the wet sand material, which can increase the amount of force to move sand granule clumps. However, it is noted that the introduction of water can lead to decreased friction between sand granules.

The performance of the system did begin to improve as the amount of water in the testbed rose, attesting to a correlation between water content and sand granule friction. Total fluidization of the area surrounding the tip of the eversion tube was achieved only after the sand being fluidized became saturated with enough water, typically requiring a layer of water an inch in depth. In addition to the noted behavior in Fiscina and Wagner, this behavior can also be explained as sand is a non-Newtonian fluid, meaning that it behaves differently than the normal assumptions made of other materials [10] [11]. Granular materials tend to act as non-Newtonian fluids in the fact that they can behave like a solid when under stress and a liquid when not [11] [12].

Despite these challenges a validated proof of soil fluidization using an underwater capable Vine Robot was achieved, the foremost priority of this research. The unique design of the system, based closely on the original Zepeda design, also proves to be a comparatively affordable platform [8]. This affordability could lend towards the ability to easily produce this design for testing and demonstration purposes.

5.2 Numerical Analysis of Water Centric Design

To properly characterize the system dynamics of the water centric design, multiple approaches to analyzing the data were conducted. The first approach looked at the relationship between growth rate of the eversion tube and the average fluidization velocity. This required amassing each trial's recorded data, a process similar to the water flow averaging seen in Section 4.5.

```
4 fluidization = []
5 For x = 1:12
6     data = 'trial' + x + 'data.txt';
7     average = mean(data);
8     fluidization(x) = average;
9 end
```

Figure 14: Pseudocode for Velocity Averaging

Twelve individual trials in the vertical testing orientation were collected. Additional time trials were tested, however, further elapsed time resulted in contact with the base of the container. This interaction caused buckling in the eversion tube, slight reversion of the eversion tube, and other complications. Due to these facts the ten second time trials were deemed to be the prime example of the system's interactions with the sand medium. Table 1 presents the numerical data related to the time trials, including both eversion length, measured after each trial, and fluidization velocity average.

Table 1: Numerical Results of Vertical Testing: Ten Second Sand Eversion

Trial	Time (sec)	Eversion Length (in)	Fluidization Rate Average (L/Hour)
1	10	10.5	104.0
2	10	9.25	113.6
3	10	9.5	102.4
4	10	9.25	108.0
5	10	10	111.2
6	10	10.75	100.8
7	10	9	95.2
8	10	6.5	99.2
9	10	7.75	97.6
10	10	8.9	91.2
11	10	10.75	95.2
12	10	9.75	95.2

In addition to the system testing data, the control experiments were measured and recorded. The results in Table 2 reflect the eversion and fluidization averages of the control experiments defined in Section 4.5.

Table 2: Numerical Results of Vertical Testing: Ten Second Control

Trial	Time (sec)	Eversion Length (in)	Fluidization Rate Average (L/Hour)
1	10	10	94.4
2	10	10.5	91.2
3	10	9.5	92.0
4	10	10.5	95.2
5	10	10.25	100.0

To determine the influence of fluidization water flow on the eversion capabilities of the system the average of both was taken for each trial. Eversion rates were determined by taking the end eversion lengths of each trial and dividing by the time it took to complete the trial. Future research into this subject could use digital position sensors to more accurately determine the eversion rates of the system. MATLAB code for eversion rate determination can be seen in Figure 15. These two values, growth rates and fluidization rates, were then plotted against one another to produce Figure 16.

```
%Determine growth rate values for each trial
tenseceversion = [10.5,9.25,9.5,9.25,10,10.75,9,6.5,7.75,8.9,10.75,9.75];
tensecgrowthrate = tenseceversion./10;
```

Figure 15: MATLAB Code for Growth Rate Determination

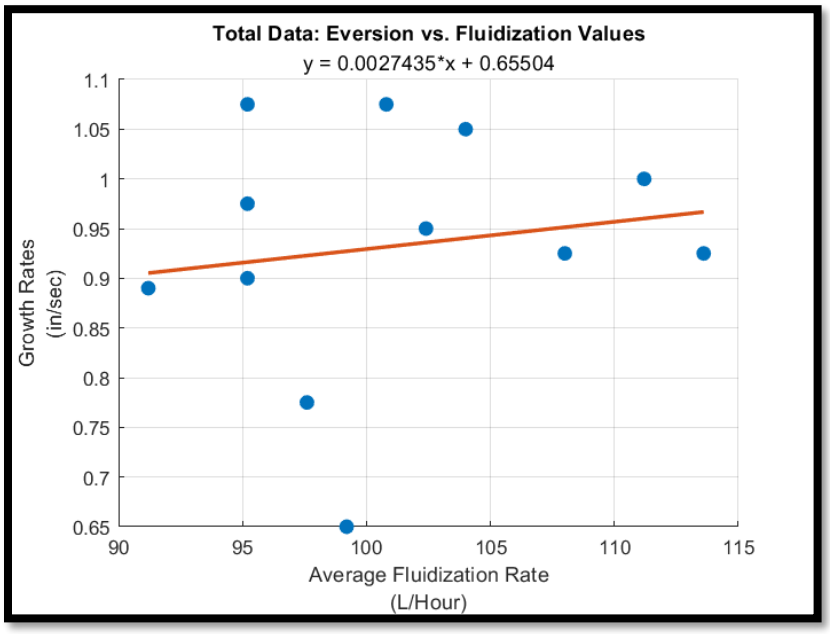

Figure 16: Growth Rate vs. Fluidization Rates – Test Data

The equation noted in the graph is the line of best fit for the scattered data points, providing one description of system dynamics. This equation is formatted as $y = mx + b$ to provide a linear description of the trend. The slope of the graph, *m*, is the scaling factor of fluidization rate to average growth rate, with the x intercept value, *b*, denoting an initial starting value to growth rates. These results show a slightly increased relationship between eversion distance over a specific time and its accompanying fluidization rate.

To further understand these values and their influence the fluidization rate can be converted into a percentage value of the total water flow. In Figure 13 the average water flow rate of the water pump was determined to be in the order of 233 [L/Hour]. With this value the average fluidization percentage could be determined. An example of how this was accomplished is seen in Figure 17.

```
nominal = #Average water flow output from pump
array = [] #Array for storing percentage values
For x = 1:12
    rate = fluidization(x); #Retrieve average fluidization rate for trial x
    percentage = rate/nominal; #Calculate percentage of water used for fluidization
    array(x) = percentage;
end
```

Figure 17: Pseudocode for percentage determination

With this code the resulting percentage values were calculated and recorded, with a numerical comparison between fluidization material velocity and the water flow output percentage seen in Table 3.

Table 3: Fluidization Percentage Values

Trial	Fluidization Rate Average (L/Hour)	Fluidization Percentage (%)
1	104.0	55.4116
2	113.6	51.2957
3	102.4	56.0976
4	108.0	53.6966
5	111.2	52.3247
6	100.8	56.7835
7	95.2	59.1845
8	99.2	57.4695
9	97.6	58.1555
10	91.2	60.8994
11	95.2	59.1845
12	95.2	59.1845

Comparing the percentage of water velocity used for fluidization to the growth rates determined earlier results in an inverse relationship to the one seen in Figure 16.

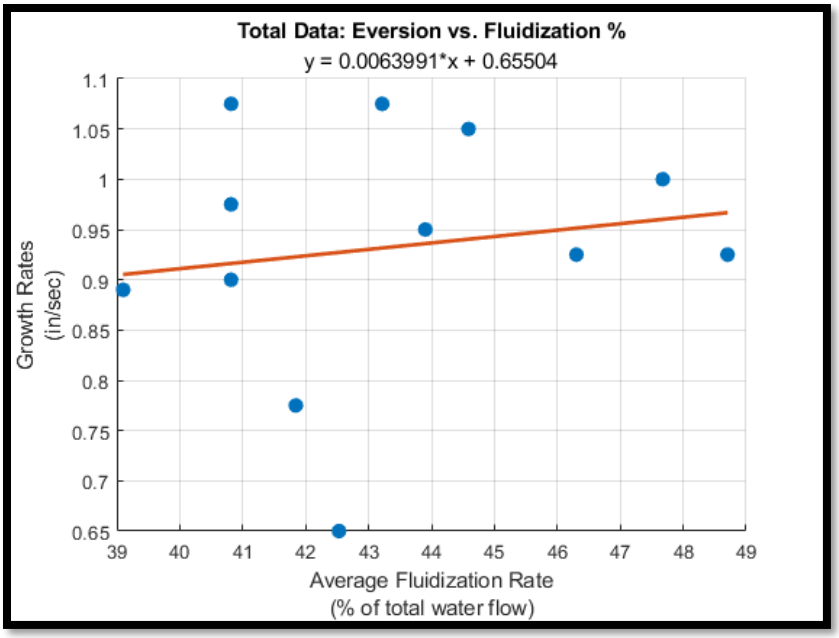

Figure 18: Growth Rate vs. Fluidization Percentage

Looking at Figure 18 it is easier to see the relationship between eversion distance and the average fluidization water flow. As the average amount of water flow directed towards fluidization increases, so does the average growth rate. However, it is important to note a large outlier to the data, which is influencing the trendline. This data point was kept in the analysis, as no outside interference on the system was observed during testing, deeming it a viable data point. However, it does present a notable difference to the main trendline of recorded data, suggesting an unseen influence such as unusual eversion stress or sensor error. If this point were removed from the dataset the relationship between growth rate and fluidization would shrink.

The control system was also tested similarly, measuring the growth rate against the average fluidization rate. In addition, the data was compared by fluidization rate and water flow percentage.

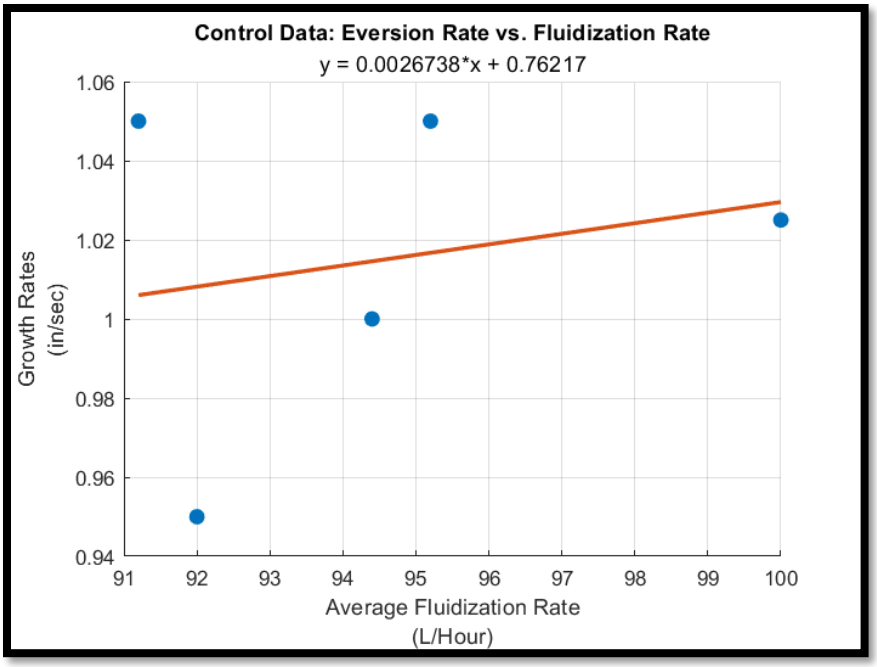

Figure 19: Control Data: Growth Rate vs. Fluidization Rate

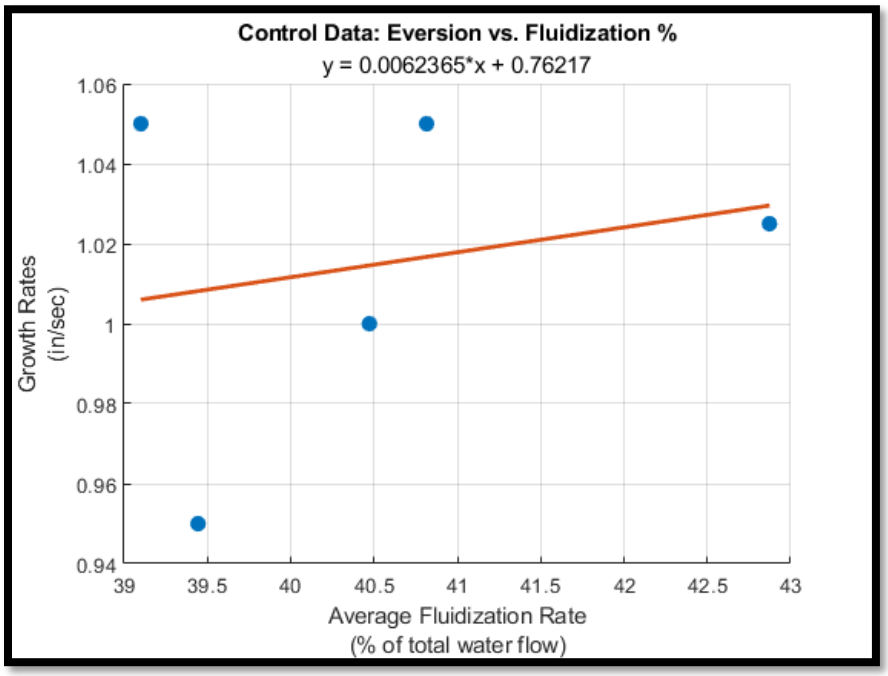

Figure 20: Control Data: Growth Rate vs. Fluidization Percentage

The relationship between eversion distance and fluidization rate is similar to the timed testing data, however with a slight decrease in slope. This can be explained as despite the fluidization line being active there is no fluidization pressure required for eversion. Given that

the control samples did not interact with the obstructing presence of sand, this graph only shows the eversion characteristics of the system in a vertical orientation, given the loss of water pressure typically used for fluidization. Without the opposing forces the sand imposes on the system, a general trend towards faster growth rates is observed.

In addition, the percentage of water flow being used for fluidization is smaller in the control data. This is likely due to back pressure caused by the force the sand presents against the eversion line in the timed trials. This pressure applied by the sand onto the eversion line would cause the incompressible water to create higher pressure in the eversion system, increasing the likelihood for the water to flow through the fluidization system as it presents less resistance. Given that the control testing did not incur this resistance, a trend towards decreased fluidization pressure is seen.

MATLAB code for numerical analysis can be found in Appendix A**: MATLAB Numerical Analysis Code** and raw numerical data used can be found in Appendix B**: Raw Measured Data**.

5.3 Theoretical Model

An attempt at creating a theoretical model for eversion speed was attempted in conjunction with another researcher, Alex Smith, to supplement the experimental data recorded during testing. This was designed using differences in pressure and friction forces inherent in the system. However, this attempt was hindered greatly by the non-Newtonian nature of wet sand as previously mentioned.

The results of this model were inconsistent with the overall results of the experimental data. For example, data retrieved from the first time trial was compared to the theoretical results, seen in Table 4.

Table 4: Theoretical vs. Experimental Velocities

Theoretical Velocity	Experimental Velocity
1.2228i m/s	0.0267 m/s

The results of the theoretical model being imaginary in nature points towards more complex physical interactions between granular materials in non-Newtonian fluids. Future research could focus on the characterization of this theoretical model in further detail. The MATLAB code used to test this model can be found in Appendix C**: MATLAB Theoretical Model Code**.

6 Conclusion

6.1 Discussion of Results

The lack of a large relationship between eversion and fluidization rates provides an intriguing discovery. This being the suggestion that the amount of fluidization material provided during testing is more than required to induce fluidization. This is due to the fact that in the testing data even the smallest average fluidization rate can provide nearly the same amount of eversion as the highest average fluidization rate. It is important to note that the largest gap between growth rates in the testing data is only a difference of 0.425 [in/sec]. In the control data this gap is smaller, 0.1[in/sec].

It is likely that decreasing values of fluidization rates could achieve the fluidization capabilities needed to allow a Vine Robot system to evert into a granular material. The system created in this project presents a basis for underwater soil fluidization and eversion. Future work could include work towards characterization of the minimum fluidization rate required to allow eversion into the sand.

In addition, it was noted that the varying levels of fluidization rates with similar eversion values could suggest that the system is self-regulating. As the pressure exerted on the eversion

arm increases, due to interaction with the sand, this could cause backflow through the water management system. In turn this backflow would direct more water to the fluidization line, given that water is incompressible and will follow the path of least resistance. As such, this would increase fluidization rates, increasing the fluidization induced in the sand that created the backflow in the first place.

6.2 Probable Sources of Error

The non-Newtonian nature makes the measurements of its impact on the eversion system difficult to properly predict. Due to this the dynamics of the system could include nonlinear features. As mentioned previously, this made creating a theoretical model of system dynamics more difficult.

The electric motor powering the water system is a Direct Current system, meaning that its output is directly affected by the supplied power. While an analog power supply was used to power the water pump, any variation in supplied power would result in variations in water output. Any changes in water output would be split between both fluidization and eversion, lowering both values and impacting the performance of the system.

As mentioned previously, testing for total water flow output of the water pump was done without the possibility of backflow or reduced operation incurred by the testing environment. It is likely that water flow output for each run could vary slightly, depending on the sand interactions and other variations in testing. A solution for this uncertainty would be to include three water flow sensors to measure each value, total output, eversion use, and fluidization use.

6.3 Future Work

Future work following this research could follow a variety of avenues. Specific focus could be given to the use of this system for underwater propulsion. The ability to grow multiple

eversion lines could be used as ‘legs’ for an underwater movement system. These legs could dig into the sand using the water fluidization demonstrated to be possible in this paper.

Another area of study could include the use of this fluidization to reach into underwater soil with a soil composition sensor affixed to the tip of eversion line. The possibility of the system being self-regulating also provides a solution to this area. If further testing shows that the system is capable of self-regulation, a relationship between backflow pressure, fluidization requirements, and soil composition could be determined.

In addition, as mentioned in Section 6.1 a study into minimum fluidization speeds to allow for eversion would help characterize the system. Specifically, a comparison between eversion tube size, fluidization rates, and the resulting eversion capabilities. It is likely as the eversion tube decreases in size the required amount of fluidization material to allow for eversion will decrease as well.

6.4 Final Remarks

The goal of the project was to design, construct, and test a Vine Robot to check the feasibility of using a soft eversion robot for soil fluidization. In this attempt a working system was achieved, and the characteristics of the system were defined in measurable values. In an underwater environment a soft eversion robot is capable of inducing sand fluidization, thereby allowing it to evert into the granular material. This achievement allows the system to explore the underwater environment to greater affect. In addition, this new capability will allow for future work to utilize the fluidization process to affect, measure, or explore underwater sand environments.

7 References

[1] E. W. Hawkes, L. H. Blumenschein, J. D. Greer and A. M. Okamura, "A soft robot that navigates its environment through growth," *Science Robotics,* vol. 2, no. 8, 2017.

[2] J. Luong, P. Glick, A. Ong, M. S. deVries, S. Sandin, E. W. Hawkes and M. T. Tolley, "Eversion and Retraction of a Soft Robot Towards the Exploration of Coral Reefs," in *2019 2nd IEEE International Conference on Soft Robotics (RoboSoft)*, Seoul, 2019.

[3] N. D. Naclerio, C. M. Hubicki, Y. O. Aydin, D. I. Goldman and E. W. Hawkes, "Soft Robotic Burrowing Device with Tip-Extension and Granular Fluidization," in *2018 IEEE/RSJ International Conference on Intelligent Robots and Systems (IROS)*, Madrid, 2018.

[4] J. D. Greer, L. H. Blumenschein, A. M. Okamura and E. W. Hawkes, "Obstacle-Aided Navigation of a Soft Growing Robot," *2018 IEEE International Conference on Robotics and Automation (ICRA),* pp. 4165-4172, 2018.

[5] J. D. Greer, T. K. Morimot, A. M. Okamura and E. W. Hawkes, "Series pneumatic artificial muscles (sPAMs) and application to a soft continuum robot," in *2017 IEEE International Conference on Robotics and Automation (ICRA)*, Singapore, 2017.

[6] L. H. Blumenschein, L. T. Gan, J. A. Fan, A. M. Okamura and E. W. Hawkes, "A Tip-Extending Soft Robot Enables Reconfigurable and Deployable Antennas," *IEEE Robotics and Automation Letters,* vol. 3, no. 2, pp. 949-956, 2018.

[7] P. Slade, A. Gruebele, Z. Hammond, M. Raitor, A. M. Okamura and E. W. Hawkes, "Design of a soft catheter for low-force and constrained surgery," in *2017 IEEE/RSJ International Conference on Intelligent Robots and Systems (IROS)*, Vancouver, 2017.

[8] J. R. Zepeda, "How to Build a Vine Robot: Pre-Formed Vine Robot," Vine Robots, June 2018. [Online]. Available: https://www.vinerobots.org/build-one/pre-formed-vine-robot/.

[9] M. M. Coad, R. P. Thomasson, L. H. Blumenschein, N. S. Usevitch, E. W. Hawkes and A. M. Okamura, "Retraction of Soft Growing Robots Without Buckling," *IEEE Robotics and Automation Letters,* vol. 5, no. 2, pp. 2115-2122, 2020.

[10] J. E. Fiscina and C. Wagner, "Wet Sand flows better than dry sand," 19 November 2007. [Online]. Available: https://arxiv.org/abs/0711.2972.

[11] H. M. Jaeger, S. R. Nagel and R. P. Behringer, "Granular solids, liquids, and gases," *Review of Modern Physics,* vol. 68, no. 4, pp. 1259-1273, 1996.

[12] S. Roy, S. Luding and T. Weinhart, "A general(ized) local rheology for wet granular materials," *New Journal of Physics,* vol. 19, p. 043014, 2017.

[13] K. N. Patil, T. J. Bowser, D. D. Bellmer and R. L. Huhnke, "Fluidization Characteristics of Sand and Chopped Switchgrass-Sand Mixtures," *Agricultural Engineering International: the CIGR,* vol. VII, 2005.

8 Appendix A: MATLAB Numerical Analysis Code

```
clear all
close all
warning('off','all')

%Load water test values
w1 = table2array(readtable("WaterTestRun1.txt"));
w2 = table2array(readtable("WaterTestRun2.txt"));
w3 = table2array(readtable("WaterTestRun3.txt"));

%Average of each water test
w1ave = mean(w1(:,2));
w2ave = mean(w2(:,2));
w3ave = mean(w3(:,2));

%Average of all water tests
wave = (w1ave+w2ave+w3ave)/3;

%Load mean values of all ten second runs
tensecarray = [];
tensecdiff = [];

%Load in Ten Second Data
for x = 1:12
    T = table2array(readtable("10secRun" + x + ".txt"));
    val = mean(T(:,2));
    diff = val/wave;
    tensecarray = [tensecarray, val];
    tensecdiff = [tensecdiff, diff];
end

%Determine growth rate values for each trial
tenseceversion = [10.5,9.25,9.5,9.25,10,10.75,9,6.5,7.75,8.9,10.75,9.75];
tensecgrowthrate = tenseceversion./10;

%Fit line to ten second data
p = polyfit(tensecarray, tensecgrowthrate, 1);
px = [min(tensecarray) max(tensecarray)];
py = polyval(p, px);

slope = num2str(p(1));
b = num2str(p(2));

%Show all ten second data
figure(1)
hold on
grid on
title("Total Data: Eversion vs. Fluidization Values")
subtitle(['y = ' slope '*x + ' b])
scatter(tensecarray, tensecgrowthrate, 60, 'filled')
xlabel({'Average Fluidization Rate','(L/Hour)'})
ylabel({'Growth Rates','(in/sec)'})
plot(px, py, 'LineWidth', 2);
```

```
%Control Method Eversion Values
controleversion = [10,10.5,9.5,10.5,10.25];

controlarray = [];
controldiff = [];

%Load in control Data
for x = 1:5
    T = table2array(readtable("10secControlRun" + x + ".txt"));
    val = mean(T(:,2));
    diff = val/wave;
    controlarray = [controlarray, val];
    controldiff = [controldiff, diff];
end

%Convert measured eversion values into in/sec values
controlgrowthrate = controleversion./10;

%Fit line to control data
p = polyfit(controlarray, controlgrowthrate, 1);
px = [min(controlarray) max(controlarray)];
py = polyval(p, px);
slope = num2str(p(1));
b = num2str(p(2));

%Show Control Data
figure(2)
grid on
hold on
title("Control Data: Eversion Rate vs. Fluidization Rate")
subtitle(['y = ' slope '*x + ' b])
scatter(controlarray, controlgrowthrate, 60, 'filled')
xlabel({'Average Fluidization Rate', '(L/Hour)'})
ylabel({'Growth Rates','(in/sec)'})
plot(px, py, 'LineWidth', 2);

disp(['Average water usage percent for fluidization is '
num2str(mean(tensecdiff)*100) ' %'])

%Convert decimal values into percentages
tensecdiff = tensecdiff*100;
controldiff = controldiff*100;

%Fit line to ten second data
p = polyfit(tensecdiff, tensecgrowthrate, 1);
px = [min(tensecdiff) max(tensecdiff)];
py = polyval(p, px);
slope = num2str(p(1));
b = num2str(p(2));

%Show ten sec eversion vs fluidization %
figure(3)
hold on
grid on
title("Total Data: Eversion vs. Fluidization %")
```

```
subtitle(['y = ' slope '*x + ' b])
scatter(tensecdiff,tensecgrowthrate , 60, 'filled')
xlabel({'Average Fluidization Rate','(% of total water flow)'})
ylabel({'Growth Rates', '(in/sec)'})
plot(px, py, 'LineWidth', 2);

%Fit line to control data
p = polyfit(controldiff, controlgrowthrate, 1);
px = [min(controldiff) max(controldiff)];
py = polyval(p, px);
slope = num2str(p(1));
b = num2str(p(2));

%Show control eversion vs fluidization
figure(4)
hold on
grid on
title("Control Data: Eversion vs. Fluidization %")
subtitle(['y = ' slope '*x + ' b])
scatter(controldiff,controlgrowthrate , 60, 'filled')
xlabel({'Average Fluidization Rate','(% of total water flow)'})
ylabel({'Growth Rates', '(in/sec)'})
plot(px, py, 'LineWidth', 2);
```

9 Appendix B: Raw Measured Data

Raw Trial Data

10secRun1		10secRun2		10secRun3		10secRun4	
Seconds	L/Hour	Seconds	L/Hour	Seconds	L/Hour	Seconds	L/Hour
1	104	1	96	1	88	1	104
2	104	2	112	2	88	2	112
3	104	3	112	3	104	3	112
4	104	4	112	4	104	4	112
5	104	5	112	5	112	5	104
6	96	6	120	6	104	6	112
7	104	7	120	7	104	7	104
8	104	8	112	8	104	8	112
9	104	9	120	9	104	9	104
10	112	10	120	10	112	10	104

10secRun5		10secRun6		10secRun7		10secRun8	
Seconds	L/Hour	Seconds	L/Hour	Seconds	L/Hour	Seconds	L/Hour
1	120	1	96	1	96	1	96
2	112	2	112	2	96	2	96
3	112	3	104	3	96	3	104
4	112	4	104	4	96	4	104
5	104	5	96	5	96	5	104
6	112	6	104	6	96	6	96
7	112	7	96	7	96	7	104
8	104	8	104	8	96	8	96
9	112	9	96	9	96	9	96
10	112	10	96	10	88	10	96

10secRun9		10secRun10		10secRun11		10secRun12	
Seconds	L/Hour	Seconds	L/Hour	Seconds	L/Hour	Seconds	L/Hour
1	80	1	48	1	56	1	48
2	96	2	88	2	96	2	104
3	104	3	104	3	104	3	96
4	104	4	96	4	96	4	104
5	96	5	96	5	96	5	96
6	104	6	96	6	96	6	104
7	96	7	96	7	104	7	96
8	96	8	96	8	104	8	104
9	104	9	96	9	96	9	104
10	96	10	96	10	104	10	96

Raw Control Data

10secControlRun1		10secControlRun2		10secControlRun3		10secControlRun4	
Seconds	L/Hour	Seconds	L/Hour	Seconds	L/Hour	Seconds	L/Hour
1	48	1	40	1	48	1	40
2	96	2	96	2	96	2	104
3	104	3	96	3	96	3	96
4	96	4	96	4	104	4	104
5	96	5	96	5	96	5	96
6	104	6	96	6	96	6	104
7	96	7	96	7	96	7	96
8	104	8	104	8	96	8	104
9	96	9	96	9	96	9	104
10	104	10	96	10	96	10	104

10secControlRun5	
Seconds	L/Hour
1	64
2	96
3	104
4	104
5	104
6	104
7	112
8	104
9	104
10	104

Raw Water Flow Data

WaterTestRun1		WaterTestRun2		WaterTestRun3	
Seconds	L/Hour	Seconds	L/Hour	Seconds	L/Hour
1	288	1	248	1	248
2	304	2	248	2	248
3	304	3	232	3	240
4	304	4	232	4	240
5	296	5	232	5	232
6	264	6	232	6	232
7	248	7	232	7	232
8	248	8	232	8	232
9	232	9	224	9	232
10	232	10	232	10	232
11	240	11	232	11	232

12	232	12	232	12	232
13	232	13	232	13	232
14	232	14	224	14	232
15	232	15	232	15	224
16	232	16	232	16	232
17	232	17	232	17	232
18	232	18	232	18	232
19	232	19	224	19	232
20	232	20	232	20	232
21	232	21	232	21	224
22	232	22	224	22	232
23	232	23	232	23	232
24	232	24	232	24	232
25	232	25	232	25	232
26	224	26	224	26	224
27	232	27	232	27	232
28	232	28	232	28	232
29	232	29	232	29	232
30	232	30	224	30	232
31	232	31	232	31	224
32	232	32	232	32	232
33	232	33	232	33	232
34	224	34	232	34	232
35	232	35	232	35	224
36	232	36	224	36	232
37	232	37	232	37	232
38	232	38	232	38	232
39	232	39	224	39	232
40	232	40	232	40	224
41	224	41	232	41	232
42	232	42	232	42	232
43	232	43	232	43	224
44	232	44	224	44	232
45	224	45	232	45	232
46	232	46	232	46	224
47	232	47	224	47	232
48	232	48	232	48	232
49	224	49	232	49	232
50	232	50	232	50	224
51	232	51	232	51	232
52	232	52	224	52	232
53	224	53	232	53	224
54	232	54	232	54	232

55	232	55	224	55	224
56	232	56	232	56	232
57	224	57	232	57	232
58	232	58	224	58	224
59	232	59	232	59	232
60	232	60	232	60	224

10 Appendix C: MATLAB Theoretical Model Code

```
%Variables
water_friction_coeff = .03;
water_density = 997; %kg/m^3
water_height = 2.5*.0254; %m
vw1 = 101.3/1000/3600/((3/16*.0254/2)^2*pi);
sand_density = 1658; %kg/m^3
sand_height = 6.5*.0254; %m
sand_friction_coeff = .4;
time = 10; %s
g = 9.79263; %m/s
eversion_length = 10.5*.0254; %m

%Calculating water pressure due to height of water
water_pressure = water_density*g*water_height;

%Calculating sand pressure due to height of sand
sand_pressure = sand_density*g*sand_height;



%Calculating Friction Pressures in Pa
%Pf12 is friction pressure through water
%Pf23 is friction pressure through sand
Pf12 = water_friction_coeff*.5*water_density*vw1^2;
Pf23 = sand_friction_coeff*(.5*water_density*vw1^2-Pf12-...
    water_pressure)

%Calculating theoretical velocity through sand in m/s
v_theoretical = sqrt((2*(.5*water_density*vw1^2-Pf12-sand_pressure-...
    -Pf23))/water_density)*sqrt(water_density/sand_density)

%Calculating experimental trial velocity in m/s
v_experimental = eversion_length/time
```